Bull. Mater. Sci., Vol. 37, No. 4, June 2014, pp. 843–848. © Indian Academy of Sciences.

Synthesis and characterization of γ-Bi_2O_3 based solid electrolyte doped with Nb_2O_5

HANDAN OZLU[1], SONER CAKAR[1,2,*], CANER BILIR[1], ERSAY ERSOY[3] and ORHAN TURKOGLU[1]

[1]Chemistry Department, Science Faculty, Erciyes University, Kayseri, Turkey
[2]Chemistry Department, Art and Science Faculty, Bulent Ecevit University, Zonguldak, Turkey
[3]Chemistry Department, Art and Science Faculty, Nigde University, Nigde, Turkey

MS received 25 April 2013; revised 14 July 2013

Abstract. **γ-phase bismuth oxide is a well known high oxygen ion conductor and can be used as an electrolyte for intermediate temperature solid oxide fuel cells (IT-SOFCs). This study aims to determine new phases of Bi_2O_3–Nb_2O_5 binary system and the temperature dependence of the electrical transport properties. The reaction products obtained in open air atmosphere were characterized by X-ray powder diffractions (XRD). The unit cell parameters were defined from the indexes of the powder diffraction patterns. The γ-Bi_2O_3 crystal system were obtained by doping 0·01 < mole% Nb_2O_5 < 0·04 at 750 °C for 48 and 96 h. Thermal behaviour and thermal stability of the phases were investigated by thermal analysis techniques. Surface and grain properties of the related phases were determined by SEM analysis. The temperature dependence of the electrical properties of γ-Bi_2O_3 solid solution was measured by four-point probe d.c. conductivity method. In the investigated system, the highest value of conductivity was observed for $\sigma_T = 0{\cdot}016$ ohm^{-1} cm^{-1} at 650 °C on 4 mole% Nb_2O_5 addition. The electrical conductivity curves of studied materials revealed regular increase with temperature in the form of the Arrhenius type conductivity behaviour.**

Keywords. **Solid electrolyte; solid state reaction; Bi_2O_3; electrical conductivity; XRD; IT-SOFC.**

1. Introduction

Solid electrolytes are the most important components of solid state electrochemical devices which are becoming increasingly important for applications in energy conversion, chemical processing, sensing and combustion control (Turkoglu and Belenli 2003). The most common solid electrolyte is stabilized zirconia, doped ceria, doped bismuth and lanthanum gallate. In recent years, many researchers have mostly focused on improving the bismuth-based electrolytes (Yılmaz *et al* 2008). Bismuth oxide (Bi_2O_3) exhibits six polymorphs: α-(monoclinic), β-(tetragonal), γ-(based centred cubic), δ-(face centred cubic), ε-(orthorhombic) and ω-(triclinic) phases and each crystalline structure exhibits different electrical behaviour (Drache *et al* 2007; Laurent *et al* 2008). α-phase is the stable phase at temperatures lower than 723 °C. The metastable β- and γ-phases are obtained by cooling down from high temperatures (Turkoglu *et al* 1998; Laurent *et al* 2008). δ-phase is only stable at temperatures between 729 and 825 °C (melting point of bismuth oxide). On cooling from high temperatures of δ-phase to room temperatures, a large hysteresis has been observed, with the possible occurrences of two intermediate metastable phases with β or γ phase (Sammes *et al* 1999). The tetragonal β-phase occurs at ~650 °C on cooling, while the γ-phase is formed at ~640 °C (Sammes *et al* 1999). Usually these metastable phases transform to the α-phase below 500 °C (Yılmaz *et al* 2008). The base centred cubic (*bcc*) γ-phase can only be obtained at room temperature and will be stable by the addition of small amount of dopant M_2O_x-type oxide, such as M = Y, Mo, V, Co, Sb, W, Sr, Ca, La and Gd (Turkoglu *et al* 1998, 2003; Sammes *et al* 1999; Drache *et al* 2007; Yılmaz *et al* 2008). The base centred cubic (*bcc*) phase is characterization of I23 space group. The investigations suggested that the γ-phase contains $Bi_{26}O_{39}$ in the cell with lattice parameters in the range of 10·10–10·27 Å. Doped γ-Bi_2O_3 phase has some defects in the crystal structure and these are described as the O^{2-} vacancy type lattice imperfections which increase with the increase of dopant rate. Takahashi and Iwahara (1978) examined electrical conductivity behaviour, ionic transfer number and phase equilibrium of Bi_2O_3–M_2O_5 (M = V, Nb and Ta) (Shannon and Prewitt 1969) and observed δ-Bi_2O_3 having high amounts of Nb_2O_5 doped additives (i.e. 10–25%).

In this study, we investigated the effect of small amounts of Nb_2O_5 doping in Bi_2O_3. After accomplishing the stability of γ-Bi_2O_3 phase, we have examined electrical,

*Author for correspondence (cakarsoner@gmail.com)

crystallographic and thermal properties of these solid electrolytes. We have determined lattice parameters at room temperature for each doped ratio of γ-Bi_2O_3 phase. We discussed effects of temperatures and doping rates on the electrical conductivity.

2. Experimental

The ceramic oxide mixtures (10 different compositions) of the $(Bi_2O_3)_{1-x}(Nb_2O_5)_x$ binary systems have been prepared in the range $0{\cdot}01 \le x \le 0{\cdot}1$ by mixing and homogenizing the stoichiometric amounts of the monoclinic Bi_2O_3 with Nb_2O_5 in an agate mortar. The starting compounds were high-purity (> 99·99% Alfa Aesar) powders. All of the solid state reactions were performed in alumina crucibles. These starting powder mixtures were calcined at 650 °C for 48 h. The grindings of the pre-annealed powder mixtures were heated up to 700 °C for 48 h, 750 °C for 48 h, 750 °C for 96 h and 800 °C for 24 h, respectively. Each thermal treatment was followed by re-grinding. At the end of each heat treatment procedure, annealed powders were slowly cooled in the furnace by switching it off (uncontrolled).

XRD was used for the preliminary investigation of all the materials synthesized to obtain phase and structure identification. Powder diffraction data of the samples were recorded with Bruker AXS D8 advanced diffractometer using Bragg–Brentano geometry with graphite monochromator CuKα radiation operated at 40 kV and 40 mA. Diffraction patterns were scanned by steps of 0·002° (2θ) over an angle range of 10–90° (2θ) and the diffracted beams were counted with a NaI(Tl) scintillation detector. The measured XRD patterns were readily compared with the reference data.

The morphology and microstructure were characterized by a LEO 440 model scanning electron microscope using an accelerating voltage at 20 kV. Microstructure measurements were made on pelletized samples at room temperature in a stainless holder 980 MPa (13 mm diameter and 1 mm thickness). Disc shaped pellets were sintered for 24 h in air at 750 °C.

For physical measurements, powder samples were pressed to pellets form at less than 980 MPa in 13 mm diameter. The pellets were then sintered by heating up to 750 °C for 10 h. The four-point probe method was the most widely used technique for electrical resistivity measurement. Two probes were used to current source and the other two probes were used to measure voltage using four probes eliminates measurement errors due to the probe resistance, the spreading resistance under each probe and the contact resistance between each metal probe and material. Fine platinum wires were directly attached to the surface of the samples to reduce the contact resistance. The ohmic characteristic of the wire contacts was checked before each measurement. The resistivity was measured in the range between ~ 200 and ~ 750 °C using Keithley 2400 source meter and Keithley 2700 multimeter which were controlled by a computer. The temperatures of the samples during conductivity measurements were measured by a thermocouple that was 2–3 mm away from the sample. This thermocouple had a cold junction at 0 °C. The temperature increments of the conductivity measurements were kept smaller as the temperature approached the phase transition temperature of the samples. The conductivity and temperature measurements were performed after thermal equilibrium had been reached.

Thermal analysis involves the measurement of sample properties as a function of temperature, rendering it a useful technique for the investigation of possible phase changes. A phase change produces either an absorption or evolution of heat. The thermal measurements were made using a simultaneous Perkin Elmer Diamond differential thermal analysis/thermogravimetry (DTA/TG) system in dynamic atmosphere using a platinum sample holder and α-Al_2O_3 inert reference substance. The specimens, usually 11–5 mg in mass, were heated at a rate of 10 °C min^{-1} from room temperature to ~ 800 °C.

3. Results and discussion

The observed single-phase and heterogeneous $(Bi_2O_3)_{1-x}(Nb_2O_5)_x$ solid mixtures, depending on the reaction temperature, is given in table 1. Samples of single phase γ-Bi_2O_3 were obtained at temperature 750 °C for 48 h and of 96 h. In this case, 750 °C was the minimum reaction temperature for γ-phase. It was obtained in the doping range $0{\cdot}01 \le x \le 0{\cdot}04$ at 750 °C, 48 and 96 h in uncontrolled cooling furnace. For these Nb_2O_5 doping ranges, all the observed XRD pattern peaks were indexed in γ-phase and δ-phase crystal system. This result showed that the low concentration doping of Nb_2O_5 into Bi_2O_3 can make easy stabilization of the γ-phase, when addition concentration of Nb_2O_5, heating temperature and heating time are correct for the formation of phase. In addition to higher doping concentration of Nb_2O_5 into Bi_2O_3 can make easy stabilization of the δ-phase. Some of the XRD patterns of the γ-phase systems are given in figure 1. On the other hand, XRD patterns of some samples could not be indexed in a single crystal system. When doping of Nb_2O_5 in the range $0{\cdot}01 \le x \le 0{\cdot}1$ was prepared for heat-treated at 700 and 800 °C, the observed individual diffraction peaks were belonging to the mixture crystal systems. These mixed phase samples and δ-Bi_2O_3 samples were excluded from this study.

As seen in table 3, theoretical (Harving 1978) and experimental 1 mole% Nb_2O_5-doped Bi_2O_3; Bragg angle (2θ), atomic lattice distance (d) value and hkl miller index were compared. This result shows that $0{\cdot}01 \le x \le 0{\cdot}04$ mole Nb_2O_5-doped Bi_2O_3 are synthesized for γ-Bi_2O_3 system.

Table 1. Observed phases in $(Bi_2O_3)_{1-x}(Nb_2O_5)_x$ systems ($0{\cdot}01 \le x \le 0{\cdot}1$).

Temperature (°C)	Mole% Nb_2O_5 addition									
	1	2	3	4	5	6	7	8	9	10
700 (48 h)	$\alpha+\gamma$	$\alpha+\gamma$	$\alpha+\gamma$	$\alpha+\gamma$	$\alpha+\gamma$	$\alpha+\delta$	$\alpha+\delta$	δ	δ	δ
750 (48 h)	γ	γ	γ	γ	$\alpha+\delta$	$\beta+\delta$	$\beta+\delta$	$\beta+\delta$	δ	δ
750 (96 h)	γ	γ	γ	γ	$\gamma+\delta$	$\beta+\delta$	$\beta+\delta$	$\beta+\delta$	δ	δ
800 (48 h)	$\gamma+\delta$	$\gamma+\delta$	$\gamma+\delta$	$\gamma+\delta$	$\gamma+\delta$	$\gamma+\delta$	$\gamma+\delta$	$\gamma+\delta$	$\gamma+\delta$	$\gamma+\delta$

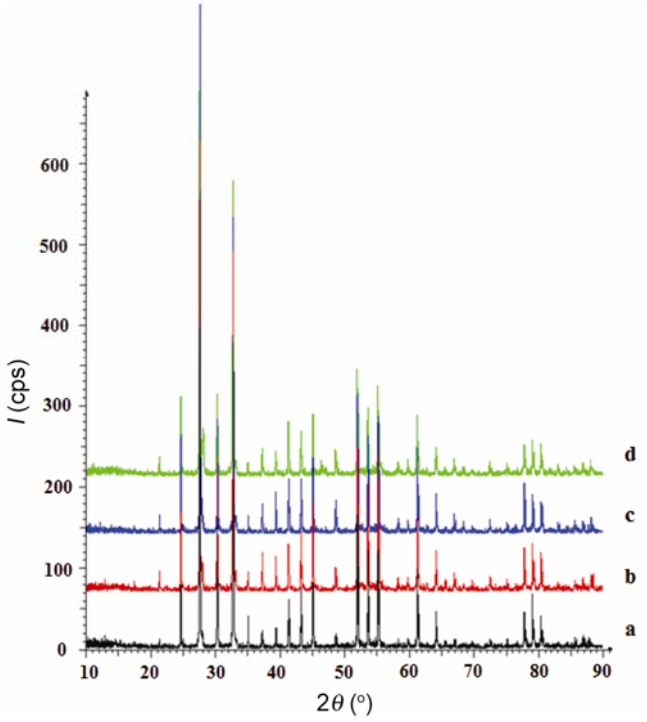

Figure 1. XRD pattern of γ-Bi_2O_3 doped with Nb_2O_5 (after heating at 750 °C for 96 h). (**a**) 1 mole%, (**b**) 2 mole%, (**c**) 3 mole% and (**d**) 4 mole%.

Table 2. Activation energy and pre-exponential factor values of γ-Bi_2O_3 solid solution doped with Nb_2O_5.

x (Nb_2O_5)	E_a (eV)	σ_0 ($ohm^{-1}cm^{-1}$)
0·01	0·304	$8{\cdot}87E^{-06}$
0·02	0·361	$1{\cdot}99E^{-05}$
0·03	0·256	$3{\cdot}14E^{-05}$
0·04	0·255	$3{\cdot}19E^{-05}$

Table 3. Calculated crystalline size for Debye–Scherrer equations of γ-Bi_2O_3 phase.

	Crystalline size	
x (Nb_2O_5)	27·42 (°)	32·65 (°)
0·01	23·696	52·779
0·02	25·295	53·669
0·03	23·418	55·165
0·04	25·504	54·781

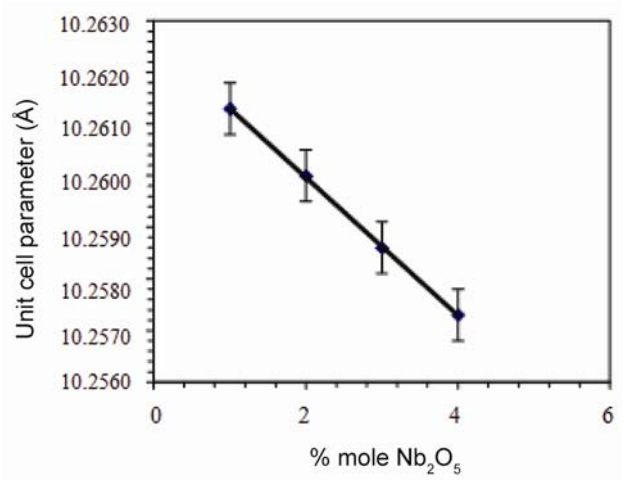

Figure 2. Relationship between Nb_2O_5 concentrations and lattice parameters of γ-Bi_2O_3.

The average crystalline size calculated for Debye–Scherrer equations is shown below:

$$D = \frac{K\lambda}{\beta\cos\theta},$$

where D is the average crystalline size, K the shape factor; the shape factor has a typical value of about 0·9, λ the X-ray wavelength; CuKα 1·542 Å, β the line broadening at half the maximum intensity FWHM and θ the Bragg angle.

The calculated unit cell parameters of the single γ-phase decrease slightly with the decrease in the addition amount of Nb_2O_5 (figure 2). The decrease of lattice parameters is in good agreement with effective ionic radii considerations. The reported ionic radii (six-coordinated) of Bi^{3+}, Nb^{3+} and Nb^{5+} cations are 1·02, 0·86 and 0·78 Å, respectively based on 1·40 Å for the O^{2-} ion (Shannon *et al* 1969; Jia 1991). When the Nb^{3+} ions replace the Bi^{3+} cations, the lattice parameter expand (Bi^{3+} ion has higher radii than Nb^{3+}) and these enlargements are consistent with our observations on the lattice parameter changes. This result also indicated that an oxidation and reduction should occur while formation of γ-Bi_2O_3 type solid solution. During this oxidation–reduction process, Nb^{5+} cations are reduced to Nb^{3+} ions, whereas O^{2-} ions in the

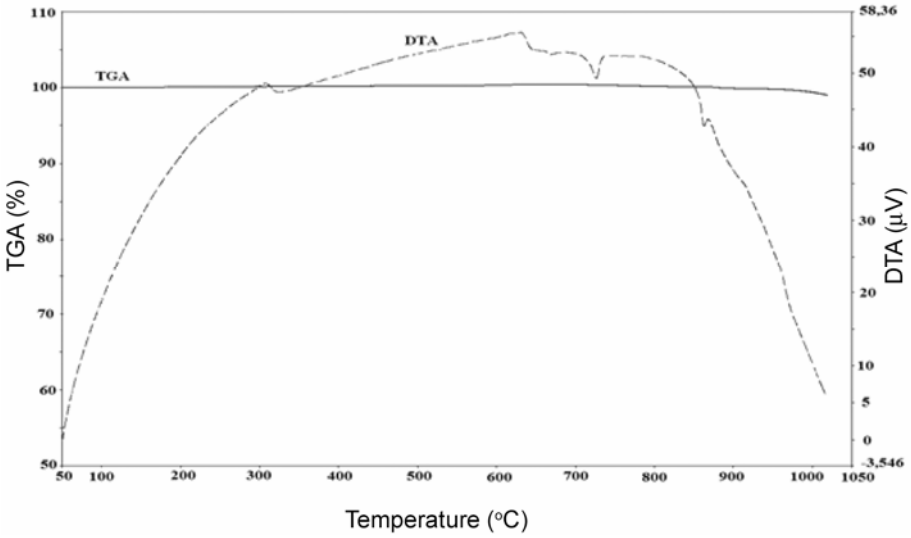

Figure 3. DTA/TG curves of 2 mole% Nb_2O_5 doped γ-Bi_2O_3.

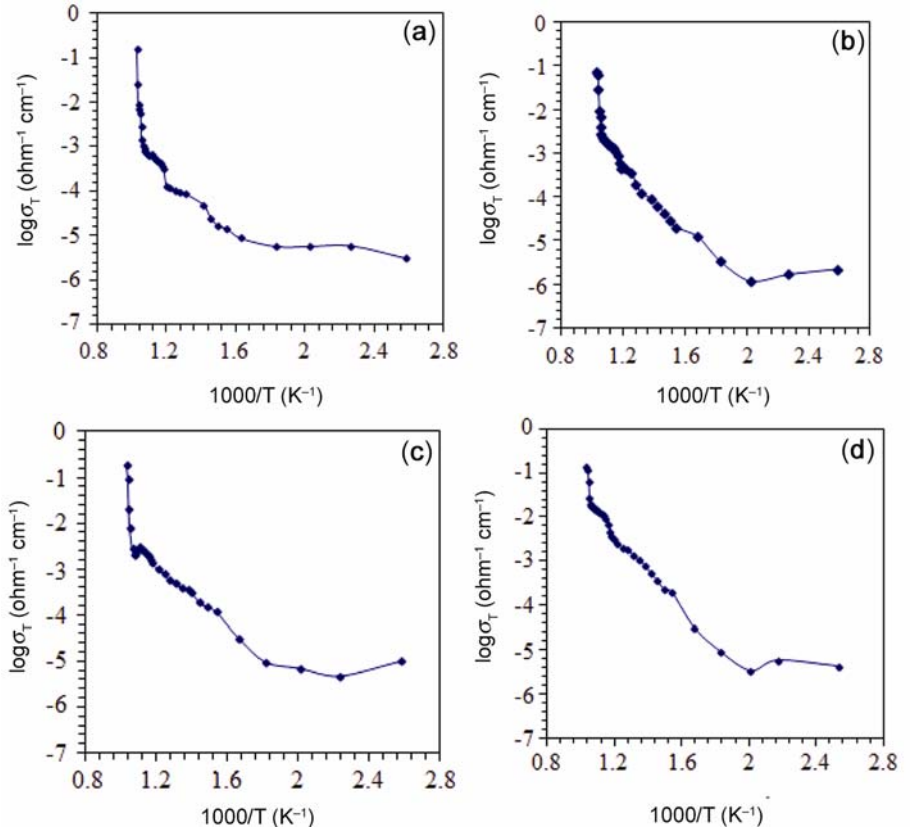

Figure 4. Temperature dependence of total electrical conductivity, σ_T of γ-Bi_2O_3 at 750 °C 96 h ((**a**) 1 mole%, (**b**) 2 mol%, (**c**) 3 mole% and (**d**) 4 mole%).

crystal lattice are oxidized to O_2 molecules. Then, some oxygen ion vacancies should occur in the O^{2-} sublattices of the γ-Bi_2O_3 solid solution.

Figure 3 shows measured DTA/TG curves of γ-Bi_2O_3 doped with 2% mole Nb_2O_5. During the heating process, a small endothermic peak on the DTA curve at ~ 750 °C was assigned to the phase transition from γ-Bi_2O_3 to δ-Bi_2O_3.

The total electrical conductivity σ_T can be determined experimentally as shown below (Bozoklu *et al* 2010):

$$\sigma_T = \sigma_0 \cdot e^{-E_a/kT}, \quad (1)$$

where E_a, T, k, σ_0 are the activation energy, temperature, Boltzmann constant and pre-exponential factor, respectively.

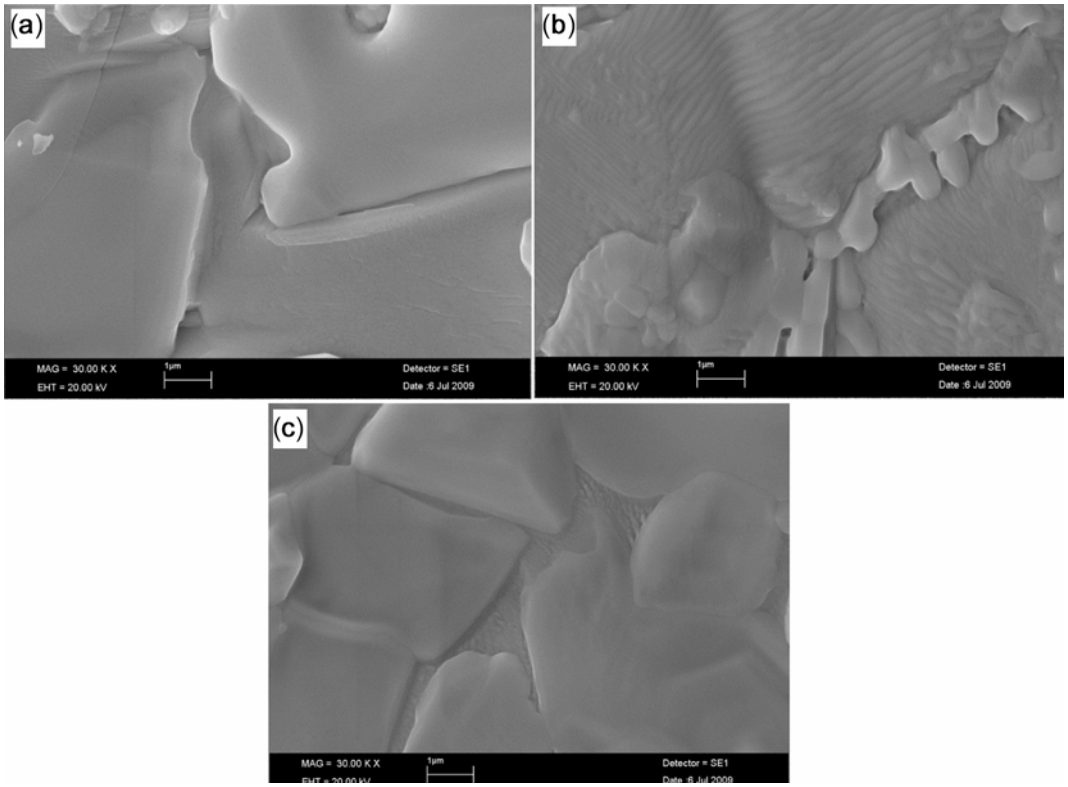

Figure 5. SEM images at γ-Bi_2O_3 for 750 °C for 96 h ((**a**) 2 mole%, (**b**) 3 mole% and (**c**) 4 mole%.

Table 4. XRD data of γ-Bi_2O_3 phase.

hkl	*d* (ref)	*d* (obs)	2θ (ref.)	2θ (obs)
900	1·12	111,954	86·907	86·952
832	1·15	113,313	84·107	85·655
830	1·18	119,281	81·505	80·449
821	1·22	122,617	78·306	77·837
810	1·25	126,278	76·306	75·180
650	1·29	130,293	73·329	72·485
700	1·44	145,047	64·678	64·155
630	1·50	151,236	61·799	61·239
533	1·54	154,640	60·026	59·752
540	1·57	158,296	58·765	58·237
610	1·65	166,384	55·660	55·157
531	1·70	170,965	53·888	53·559
530	1·74	175,888	52·553	51·946
520	1·86	187,221	48·930	48·591
500	2·02	201,117	44·833	45·041
422	2·08	209,367	43·473	43·175
332	2·17	218,598	41·584	41·266
420	2·27	229,295	39·673	39·260
330	2·41	241,742	37·281	37·162
400	2·54	256,305	35·308	34·980
321	2·73	274,037	32·778	32·651
222	2·94	295,940	30·378	30·174
310	3·22	324,147	27·681	27·494
220	3·60	362,329	24·71	24·549
211	4·20	418,862	21·136	21·194

The slope of the linear part of the Arrhenius curve in the '$\ln(\sigma_T) - 1/T$' graph is equal to $-E_a/k$. It is extensively reported that it indicates a change or a phase transition in the conductivity mechanism (Yılmaz *et al* 2008; Bozoklu *et al* 2010). For the temperature range, where γ-form is present '$\log(\sigma_T) - 10^3/T$' relation is linear. From the Arrhenius curves drawn for all samples, the activation energy E_a is calculated (table 2). The ionic conductivity of the pellet samples was analysed by a four-probe method in the temperature range from 50 to 800 °C. '$\log(\sigma_T)$–$10^3/T$' graphs are drawn in order to show the conductivity change with respect to temperature. The graphs are compared with each other and the conductivity characteristics of the sample are evaluated. Electrical conductivity plots for 1–4 mole% (750 °C, 96 h) γ-Bi_2O_3 are given in figure 4. Plots of other single γ-phase samples were quite similar to the plots given in these figures. As seen in these figures, the conductivity of all the samples increases with increasing temperature. It was proposed that this is connected with the interstitial oxygen ionic mobility which rises with temperature. The number of charge carriers and mobility make an increment result for the total electrical conduction. At elevated temperatures, thermal activation of the O^{2-} ions increases, resulting in higher oxygen ion movement rate. Additionally, the concentration of thermally-induced O^{2-} vacancies can increase with temperature and these formations of vacancies can make a positive result for electrical conduction. Although, interstitial oxygen vacancies are present in the γ-Bi_2O_3 structure at low temperatures, thermal energy of

the charge carrier is not enough for jumping to the nearest neighbour interstitial O^{2-} vacancy lattice positions. The lower mobility of carrier at low temperatures, causes movement of the oxygen ions, then reduce electrical conductivity. At high temperatures, thermal vibrations of carriers may also assist the jumping process momentarily by either shortening the jumping distances or by widening the jumping conducting paths through the crystal lattice. On the other hand, the disordered arrangements of the vacancies in the interstitial O^{2-} sublattice, which are along some special directions in the *bcc* unit cell, may occur at high temperatures. This greater degree of disorder structure can also play an important role for exhibiting of higher mobility, easier movement of carriers and the increment of the electrical conduction with temperature.

As seen in figure 5, SEM image of the pellet samples and fracture surfaces showed a grain size of $\sim 10\ \mu$m. SEM image shows sharper grain boundaries of samples. Sharpness of the grain boundaries gradually increases grain connectivity and this results in increasing conductivity.

In addition to electrical conductivity graphs, 730–750 °C is seen as a sudden rise. Sudden change in conductivity and DTA/TG measurements determined from γ-Bi_2O_3 to δ-Bi_2O_3 resulted in phase transformation. DTA/TG and conductivity measurement results proved to be in agreement.

4. Conclusions

The metastable γ-phase of Bi_2O_3 and δ-phase of Bi_2O_3 solid solution have been obtained at room temperature by doping of Nb_2O_5 into the pure monoclinic α-Bi_2O_3 and employing solid state reaction. Nb^{3+} cations substituted Bi^{3+} cations in the crystal structure of γ-phase. The results of XRD, DTA/TG measurements were in agreement with the results of the observed electrical conduction values. Heat treatment temperatures, heating period, cooling rates, mechanical regrinding and doping amount of Nb_2O_5 are effective factors for the crystallographic and electrical conductivity properties of the produced body centred cubic Bi_2O_3 type solid electrolyte system.

Acknowledgements

The authors would like to thank the Scientific and Technical Research Council of Turkey (TUBİTAK) for financial help (Grant no. 108T377).

References

Bozoklu M, Turkoglu O, Yilmaz S, Ari M and Belenli I 2010 *Mater. Sci. Technol.* **26** 1239

Drache M, Roussel P and Wignacourt J P 2007 *Chem. Rev.* **107** 80

Harwig H A 1978 *Z. Anorg. Allg. Chem.* **444** 151

Jia Y Q 1991 *J. Solid State Chem.* **95** 184

Laurent K, Wang G Y, Tusseau-Nenez S and Leprince Wang Y 2008 *Solid State Ionic.* **178** 1753

Sammes N M, Tompsett G A, Nafe H and Aldinger F 1999 *J. Eur. Ceram. Soc.* **19** 1801

Shannon R D and Prewitt C D 1969 *Acta Crystallogr.* **25** 925

Takahashi T and Iwahara H 1978 *Mater. Res. Bull*. **12** 1447

Turkoglu O and Belenli I 2003 *J. Thermal Anal. Calor.* **73** 1001

Turkoglu O, Gumus A and Belenli I 1998 *Balkan Phys. Lett.* **6** 34

Yılmaz S, Turkoglu O and Belenli I 2008 *Mater. Chem. Phys.* **112** 472